Model under-representation of decadal Pacific trade wind trends and its link to tropical Atlantic bias

Jules B. Kajtar*[1,2,3] (orcid.org/0000-0003-0114-6610), Agus Santoso[1,2] (orcid.org/0000-0001-7749-8124), Shayne McGregor[1,4] (orcid.org/0000-0003-3222-7042), Matthew H. England[1,2] (orcid.org/0000-0001-9696-2930), and Zak Baillie[1,2]

[1] Australian Research Council's Centre of Excellence for Climate System Science, Australia

[2] Climate Change Research Centre, University of New South Wales, NSW, Australia

[3] College of Engineering, Mathematics, and Physical Sciences, University of Exeter, Exeter, UK

[4] School of Earth, Atmosphere and Environment, Monash University, Victoria, Australia

* Corresponding author: Jules B. Kajtar; j.kajtar@exeter.ac.uk. Now at College of Engineering, Mathematics, and Physical Sciences, University of Exeter, Exeter, UK

Keywords: Pacific trade winds, decadal variability, Walker Circulation, CMIP5

Acknowledgements

This study was supported by the Australian Research Council. We acknowledge the World Climate Research Programme's Working Group on Coupled Modelling, which is responsible for the Coupled Model Intercomparison Project (CMIP), and we thank the climate modelling groups for producing and making their model output available. We also acknowledge the observational reconstructions provided by the Hadley Centre (HadISST), NOAA/OAR/ESRL PSD (20th Century Reanalysis, ERSST and NCEP/NCAR Reanalysis), and ECMWF (ERA-20C).

Abstract

The strengthening of the Pacific trade winds in recent decades has been unmatched in the observational record stretching back to the early twentieth century. This wind strengthening has been connected with numerous climate-related phenomena, including accelerated sea-level rise in the western Pacific, alterations to Indo-Pacific ocean currents, increased ocean heat uptake, and a slow-down in the rate of global-mean surface warming. Here we show that models in the Coupled Model Intercomparison Project phase 5 (CMIP5) underestimate the observed range of decadal trends in the Pacific trade winds, despite capturing the range in decadal sea surface temperature (SST) variability. Analysis of observational data suggests that tropical Atlantic SST contributes considerably to the Pacific trade wind trends, whereas the Atlantic feedback in coupled models is muted. Atmosphere-only simulations forced by observed SST are capable of recovering the time-variation and the magnitude of the trade wind trends. Hence, we explore whether it is the biases in the mean or in the anomalous SST patterns that are responsible for the under-representation in fully coupled models. Over interannual time-scales, we find that model biases in the patterns of Atlantic SST anomalies are the strongest source of error in the precipitation and atmospheric circulation response. In contrast, on decadal time-scales, the magnitude of the model biases in Atlantic mean SST are directly linked with the trade wind variability response.

1. Introduction

The Pacific trade wind strengthening in recent decades has been unprecedented in the observational record stretching back to the late 19th century (L'Heureux et al. 2013). The acceleration has been proposed as the mechanism behind the early 21st century global surface warming slowdown (England et al. 2014). In this mechanism, heat uptake is increased through the acceleration of the wind-driven ocean overturning circulation, and the subducted heat is accumulated in the western Pacific (England et al. 2014) before being transported to the Indian Ocean via the Indonesian Throughflow (Lee et al. 2015). These upper ocean circulation changes have altered the pattern of sea surface temperature trends over the Pacific Ocean. Given the profound climatic impacts associated with a redistribution of heat in the upper ocean, understanding the drivers of Pacific trade wind variability is essential for interannual and decadal climate predictions and monitoring.

The Pacific trade winds are the surface level expression of the Pacific Walker Circulation cell (e.g. Gill 1980). This cell encompasses an ascending branch over the Maritime Continent, prevailing westerly winds in the upper troposphere, a descending branch over the eastern Pacific, and the trade winds that extend across the surface of the equatorial Pacific Ocean. Possible reasons for the unprecedented trade wind acceleration during the early 21st century – beyond that due to the negative phase of the Interdecadal Pacific Oscillation (IPO; England et al. 2014) – include contributions from aerosol forcing (Takahashi and Watanabe 2016), and sea surface warming trends over the Indian Ocean (Luo et al. 2012; Mochizuki et al. 2016), or Atlantic (Kucharski et al. 2011; McGregor et al. 2014; Chikamoto et al. 2016; Kucharski et al. 2016a; Kucharski et al. 2016b; Li et al. 2016; Ruprich-Robert et al. 2016), or both (Zhang and Karnauskas 2017). Using atmospheric model experiments forced with SST trends, McGregor et al. (2014) and Li et al. (2016) argued that the Atlantic warming is more important than the Indian Ocean warming, although tropical interactions across the three ocean basins can be quite different across different time-scales (Kajtar et al. 2016; Kucharski et al. 2016b). Specifically, El Niño tends to heat the Indian and Atlantic basins on interannual time-scales (Lau and Nath 1994), whereas Indian and Atlantic SST trends tend to influence the Pacific on multi-decadal time-scales (e.g. Li et al. 2016). Coupled models may be deficient in this regard, with eastern Pacific SST apparently overly constraining the global mean climate (Douville et al. 2015). However, the model mismatch on decadal variability does not appear to have implications for future projections (England et al. 2015).

The recent trade wind acceleration is in apparent contrast to the projected weakening of the Walker Circulation under greenhouse warming (Vecchi et al. 2006; Vecchi and Soden 2007). Power and Kociuba (2011) showed that models and observations tend to be in agreement regarding the weakening trend of the Walker Circulation over the 20th Century, and external forcing has been estimated to account for about half of the change. Yet recent studies (e.g. England et al. 2014; Kociuba and Power 2015) show that historical and pre-industrial model simulations participating in the Coupled Model Intercomparison Project, phase 5 (CMIP5) appear unable to reproduce anywhere near the magnitude of the recent observed trends. The reasons behind this shortcoming in models remains unclear. Motivated by the importance of the Pacific trade winds on global climate, our study aims to explore the contribution of Atlantic Ocean SST variations on Pacific trade wind trends in climate models. We find that biases in the patterns of Atlantic SST anomalies, as well as the mean Atlantic SST distribution, likely inhibit the tropical Atlantic connection to the central Pacific on decadal time-scales in CMIP5 models. An understanding of the nature of these biases will thus ultimately help to explain the underestimation of the Pacific trade wind variability in models, and lead to improved multi-year forecasting skill (Chikamoto et al. 2015).

The rest of this paper is divided as follows. After outlining the data and methods in Section 2, the decadal wind stress and SST trends in observations and models, and the relationships between them, are analysed in Section 3. We then explore the notable differences in the Atlantic feedback in models as compared to observations (Section 4), before delving into an analysis of the source of the atmospheric response bias in models (Section 5).

2. Data and methods

In this study, we focus on the drivers of Pacific trade winds trends over the 20th and early 21st century, in observations and the historical CMIP5 simulations. Since most historical simulations end at year 2005, we extend them with the RCP8.5 scenario simulations to cover a common time-span of 1900 to 2014 amongst all models and reanalysis products. The choice of RCP extension does not make a significant difference for this early period of the 21st century (e.g. England et al., 2015). Using only the "r1i1p1" experiments, models that do not span from the year 1900, or do not have an appropriate RCP8.5 extension, are not included. The

three variables analysed herein were sea surface temperature (CMIP5 variable name: tos), wind stress (tauu), and rainfall (pr). Later we also analyse the Atmospheric Model Intercomparison Project (AMIP) r1i1p1 simulations, which were run with observed SST forcing, but this experiment is available for fewer models, and only over the period 1979 to 2008.

The observed data was gathered from the HadISST (Rayner et al. 2003), NOAA-20CR v2c (Compo et al. 2011) and ERA-20C (Poli et al. 2016) reanalysis products. The HadISST sea surface temperature is analysed together with the NOAA-20CR wind stress and precipitation, whereas the ERA-20C product has all three variables available. Again, we choose a common period of 1900 to 2014, with the exception of ERA-20C, which ends at 2010. The NOAA-20CR/HadISST and ERA-20C reanalysis products provide the observational basis for our model comparison throughout, but for validation purposes, we initially compare sea surface temperature trends to ERSST v4 (Huang et al., 2014) and wind stress trends to NCEP/NCAR Reanalysis 1 (Kalnay et al. 1996).

Most of the following analysis is of running 10-year trends, but where we use annual data, the 11-year running mean is first removed from the time-series to nullify lower frequency variability. All quoted values of correlation are the Pearson's correlation coefficient.

3. Decadal wind stress and SST trends in observations and models

Observed zonal wind stress variability across the equatorial Pacific tends to be greater in the west, peaking near the dateline, as shown by the standard deviation of the annual data and 10-year trends in the reanalysis products (Fig. 1a, b). The CMIP5 models exhibit a large distribution, and while most models do simulate the stronger variability in the west, the ensemble mean peak in variability is too far to the east, and the overall magnitude of variability, particularly over decadal time-scales, is underestimated. This model deficiency is further highlighted in the range of the 10-year trends in τ_{PAC}, an index of zonal wind stress averaged over 160°E – 150°W and 8°S – 8°N (Fig. 1c). Although some models simulate the observed extreme positive trends (i.e. trade wind decelerations), none capture the range, nor the extreme negative trends observed in recent decades (i.e. the recent trade wind acceleration). Note however that the two reanalysis products are not completely consistent with each other, with the NOAA-20CR trends showing larger range than those calculated using ERA-20C. This difference is primarily due to a strong negative trend in NOAA-20CR in the

early 20th Century (Fig. S1), but these early observations tend to be less reliable. To check the consistency among observations, we introduce the NCEP/NCAR reanalysis wind stress. There is reasonable agreement in the 10-year trends of the Pacific wind stress index (Fig. S1a), and the running correlations between them tend to improve with time (Fig. S1c). The NCEP/NCAR reanalysis is not used in the remainder of this study due to its shorter time coverage (it starts in 1948).

McGregor et al. (2014) showed that the Atlantic-Pacific SST see-saw is a strong driver of the Pacific trade winds. More specifically, they revealed a strong correlation between the "trans-basin variability (TBV) index" and western Pacific wind stress. The TBV is defined as the difference between the area-averaged Atlantic SST (ATL; 70°W–20°E) minus Pacific SST (PAC; 120°E–90°W). It will be shown later that tropical SST between 20°S–20°N contributes most strongly to the central Pacific wind stress trends, hence the choice here to restrict the TBV index to this meridional range (in contrast to McGregor et al. 2014, who use the domain 30°S–60°N). The two observational products show stronger agreement in the TBV trends compared with the τ_{PAC} trends (Fig. 2a), most likely because the TBV is an area-average over a much larger region. But to provide further validation, we introduce the ERSST product. There is agreement between all three sets (Fig. S1b). Again, the running correlations tend to improve over time (Fig. S1d), although the world-war I and II periods are marked by sharp declines, most likely due to sparser observations. The HadISST climatology is used in favour of ERSST from this point on, primarily because it is of higher resolution. Overall, the CMIP5 models appear to capture the observed variability of the TBV index, as well as the Pacific and Atlantic components separately (Fig. 2). The multi-model range in 10-year trends of the TBV index compares well with the observed, although individual models exhibit different levels of variability (Fig. 2a). Somewhat surprisingly, the 5% to 95% range in the multi-model distribution of 10-year trends in PAC spans a larger range than the observed (cf. black and grey bars, Fig. 2b), however the number of sampled decades is of course much larger in the multi-model set compared to the individual observed realisations.

The trans-basin SST gradient correlates strongly with western Pacific wind stress at the annual time-scale in observations (McGregor et al. 2014). For our TBV narrowed to the tropics, the correlation with the wind stress is stronger for decadal trends than with annual data (namely, -0.84 compared with -0.76 for NOAA-

20CR, and -0.75 compared with -0.58 for ERA-20C). Despite the deficiency in simulating the observed τ_{PAC} variability (Fig. 1), the models nevertheless capture the decadal TBV-τ_{PAC} correlation reasonably well (Fig. S2), although the multi-model ensemble correlation is slightly underestimated. In terms of the sensitivity of the wind stress trends to the TBV, almost all the models also underestimate compared to the observed relationships (Fig. 3a). This indicates that the smaller range of Pacific wind trends in the models could be due to a weaker coupling between the winds and the SST gradient across the Pacific-Atlantic basins. Further examination of the individual TBV components reveals that the models perform well in capturing the observed correlation between the wind and the PAC SST index (Fig. S2). Although the models are again consistent in the sign of the regression, the apparent degree of coupling is also underestimated (Fig. 3b). In stark contrast, the relationship between Pacific zonal wind stress and the ATL index shows a large disparity between models and observations (Fig. S2, 3c), with inconsistent sign in the correlations across models. Twelve models exhibit statistically significant positive correlations, (i.e. warm Atlantic SST trends correspond with westerly Pacific wind stress trends), and the rest of the models show statistically insignificant correlations. In contrast, the NOAA-20CR τ_{PAC} correlation with HadISST ATL is negative and statistically significant. The ERA-20C negative correlation is not statistically significant over the entire 20th century period, but the agreement with NOAA-20CR improves over more recent decades. For example, over the period 1970 to 2014, the regression between 10-year trends in τ_{PAC} and ATL is -0.034 N m^{-2} K^{-1} ($p<0.01$) for NOAA-20CR and -0.030 N m^{-2} K^{-1} ($p<0.01$) for ERA-20C.

Since the Indian Ocean is known to influence the Pacific on decadal time-scales (Luo et al. 2012; Li et al. 2016; Mochizuki et al. 2016; Zhang and Karnauskas 2017), it is instructive to explore the relationship between Indian Ocean SST (IND; averaged over 20°S–20°N and 40°E–120°E) and the Pacific wind stress index. As with the TBV and PAC indices, but aside from a small number of exceptions, the models are overall consistent with observations with regard to the relationship between τ_{PAC} and IND (Fig. S3).

It is clear that overall the Pacific component of the TBV is more strongly connected with decadal Pacific wind stress trends than the Atlantic, or indeed with the Indian Ocean. For example, in the NOAA-20CR product, the Pacific wind stress response is 0.35 N m^{-2} K^{-1} to PAC (Fig. 3b) compared with -0.17 N m^{-2} K^{-1} to ATL (Fig. 3c). But the unprecedented 1992 to 2011 equatorial Pacific wind stress trend was not consistent

185 with a Pacific-only SST driving mechanism (England et al. 2014). The Atlantic SST trend seems to have
186 been crucial for the unprecedented trade wind trends (McGregor et al. 2014; Chikamoto et al. 2016), and in
187 fact the Atlantic may be the most consistent remote driver of tropical SST variability (Li et al. 2016;
188 Kucharski et al. 2016b). The differences across the models and with observations seen in Fig. 3c motivate
189 further examination on the implications of the inconsistent Atlantic feedback on the Pacific wind-stress
190 trends via the TBV. The Indian Ocean is not explored further, since, as noted earlier, the models largely
191 behave consistently with observations in that connection.
192
193 **4. Contribution of tropical Atlantic SST bias**
194 Over interannual time-scales, the Atlantic component tends to dominate the TBV index (McGregor et al.
195 2014), and this relationship persists for the re-defined TBV domain used in this study. On decadal time-
196 scales, the Atlantic component continues to play a strong role, although its contribution to the TBV is
197 slightly weaker than the Pacific component (in observations; Fig. 4a). The models, on the other hand, tend to
198 show a weaker TBV contribution from the Atlantic (see MMM, Fig. 4a). The correlations across models
199 suggest that where the Atlantic SST trends contribute more strongly to the TBV, the correlation between the
200 ATL index and τ_{PAC} trends tend to be more negative (Fig. 4b). In other words, where there is a stronger
201 Atlantic contribution to trans-basin SST variability in models, warm Atlantic SST trends are more strongly
202 connected with enhanced Pacific trade wind trends, as seen in observations. Similarly, the inter-model
203 analysis shows that stronger correlations between PAC and TBV trends tend to occur with stronger
204 correlation between PAC SST and τ_{PAC} trends (Fig. 4c). It is important to again emphasise that among
205 models, the ATL and τ_{PAC} correlation is less consistent with observations than the PAC and τ_{PAC} correlation.
206 This strong inter-model disagreement, but statistically significant relationship (Fig. 4b), motivates the
207 analysis of Pacific wind trend responses specifically to Atlantic SST trends in models.
208
209 The regressions of running 10-year τ_{PAC} trends with SST reveal an Interdecadal Pacific Oscillation (IPO)
210 signature that is similar in the multi-model mean (Fig. 5a) and the two reanalysis products (Fig. 5c, e).
211 Models perform reasonably well in simulating the IPO (Henley et al. 2017), and so this robust connection to
212 the Pacific trade wind trends is not surprising. Differences between the modelled and observed regression
213 patterns are nevertheless apparent. For instance, the τ_{PAC} trends in observations are more sensitive than in

models to SST trends over the Pacific and Indian Oceans, including the Maritime Continent. But despite the differences in magnitude in these regions, the multi-model regressions are at least of the same sign as the observations. This is in stark contrast to the Atlantic, where the regression pattern is entirely different in the models and observations. Namely, there is a statistically significant positive signal in the southern tropical Atlantic in the multi-model mean, while the observations display a statistically significant negative signal. It is known that the CMIP5 models exhibit strong biases in the southern tropical Atlantic, and the biases originate from a range of possible sources (e.g., Toniazzo and Woolnough 2014). The observations reveal an Atlantic meridional dipole signature, and although the positive signal emerges in the northern tropical Atlantic in the model mean, it is confined closer to the equator. The Atlantic dipole pattern in observations, however, does not give a complete picture, since this regression analysis treats each spatial point independently of its neighbours. We have performed a multiple linear regression analysis to re-construct the τ_{PAC} trends from SST trends alone, which incorporates the area-average SST trends of the Pacific, and the South and North Atlantic Ocean regions, as three separate terms. In that reconstructed expression, the coefficients for the North and South Atlantic terms carry the same sign. In other words, when considering the Atlantic SST influence on the Pacific trade wind trends, our choice of using the ATL region is appropriate, and does not need to be split further into northern and southern components to capture opposite signs, as might have been inferred from Fig. 5c, e.

Considering the different τ_{PAC} trend responses to Atlantic SST trends among models and observations (Fig. 3c), we now examine the atmospheric response, specifically rainfall, to Atlantic SST trends. Interestingly, there is stronger agreement between the models and observations for the τ_{PAC} trends regressed with precipitation trends across the tropical Atlantic (Fig. 5b, d, e). In particular, the negative signals denote decreasing Atlantic precipitation trends in association with westerly τ_{PAC} trends. This precipitation linkage reflects Atlantic convection changes and their associated impact on the Pacific Walker circulation (McGregor et al. 2014). Surprisingly, the decreased precipitation over the tropical Atlantic (Fig. 5b) does not appear to be consistent with local warming trends in the models (Fig. 5a). This is unlike the observations in which reduced precipitation (Fig. 5d, f) can be seen as a physically consistent response to local sea surface cooling (Fig. 5c, e; more clearly seen in the southern tropical Atlantic). Finally, it is interesting to note that

the familiar double-intertropical convergence zone (ITCZ) is apparent in the multi-model mean even on this decadal time-scale (Fig. 5b; Lin 2007).

The Atlantic Ocean model discrepancy can be explored further by examining the responses to Atlantic SST trends, as done by regressing the ATL index onto grid-point SST and rainfall (Fig. 6). This analysis shows that, unlike in the observations (Fig, 6d, f), the precipitation response over the tropical Atlantic in the multi-model mean is very weak, with little stippling (Fig. 6b), despite similarities in the SST patterns (cf. Fig. 6a and Fig. 6c, e; albeit weaker in the multi-model mean). This indicates that either the Atlantic precipitation response is too weak in each of the models, or that large inter-model diversity tends to cancel out positive and negative responses in the multi-model mean. Either way, the modelled precipitation response in the tropical Atlantic appears to respond more consistently to the tropical Pacific warming (which induces subsidence and therefore drying on the Atlantic side), rather than local SST trends (cf. Fig. 5b and Fig. 6b). In this way, the models seem to simulate overly strong remote forcing of the Atlantic by Pacific SST, and too little forcing of the Pacific by Atlantic SST. It will be shown later that the Atlantic precipitation response to local SST is even weaker on the annual time-scale. In terms of the Pacific response, the models show increasing central Pacific precipitation (Fig. 6b), which is consistent with the Pacific warming (Fig. 6a). The observed analyses (Fig. 6d, f) on the other hand show decreasing central Pacific precipitation, consistent with either Pacific cooling or Atlantic warming, both of which are known to induce atmospheric subsidence over the Central Pacific (McGregor et al. 2014; Chikamoto et al. 2016; Li et al. 2016). Since precipitation is a proxy for convection, these results indicate that the models are deficient in simulating convective processes over the tropical Atlantic. If convection is muted, then so too will be the influence of the Atlantic on the descending branch of the Pacific Walker Circulation cell, thus leading to weaker Atlantic influence on the surface level expression of the Walker Circulation, namely the Pacific trade winds. Hence our findings indicate that the Atlantic-Pacific connection in the models is not consistent with observations. It is likely due to biases in the Atlantic region that appear to limit the response of the atmospheric circulation and convection to the underlying SST anomalies.

5. Possible causes of atmospheric response bias

To further elucidate the nature of the biases in the coupled models, we first consider whether similar issues also exist in atmospheric-only simulations. Here we examine the Atmospheric Model Intercomparison Project (AMIP) simulations from the CMIP5 model set. The AMIP experiments are simulated with observed global SST fields, but they are only available for much shorter period (1979 to 2008), and with fewer models. With prescribed observed SST fields, variability in Pacific wind stress is greatly enhanced, at both the annual (Fig. 7a) and decadal (Fig. 7b) time-scales. Where previously in the historical coupled simulations the variability was weaker-than-observed across all models (Fig. 1), here in the AMIP simulations it is greater in many models. Although different biases now become apparent, particularly the overly strong variability signal over the Pacific warm pool. The time-series of 10-year τ_{PAC} trends shows that the variations in models are synchronized with observations, despite the differences in magnitudes (Fig. 7c). Thus, the strong biases that are apparent in the coupled simulations are muted in the atmosphere-only simulations forced by observed SST, and hence the multi-model ensemble range in 10-year τ_{PAC} trends is greatly improved (Fig. 7d; Ma and Zhou 2016). The regression fields of τ_{PAC} trends with SST and precipitation are in significantly greater agreement with observations in the AMIP runs (Fig. 8) compared to the fully coupled historical runs (Fig. 5). Likewise, the AMIP precipitation trend over the Atlantic is in good agreement with observations (cf. Fig. S4 with Fig. 6b, d, f). Finally, there are some differences in the fields over the two time-periods analysed in the observations, most notably over the Indian and North Atlantic Oceans (cf. Fig. 5c–f and Fig. 8c–f), but these differences may be related to multi-decadal variability (Kucharski et al. 2016a).

In order to understand why the coupled models do not appear to generate the correct decadal precipitation response to Atlantic SST (Fig. 6b, d, f), we regress the annual ATL index with precipitation (Fig. 9) and compare this response to anomalous SST patterns (Fig. S5). For this analysis, the 11-year running mean is removed from the annual time-series, for all indices and at each spatial point in the field variables. In the observations, it is apparent that the precipitation anomalies are bounded by the 27.5° C isotherm of the climatological SST, and the same isotherm of the anomalous plus climatological SST field (Fig. 9b, c), consistent with theory (e.g., Graham and Barnett 1987; Zhang 1993; Sud et al. 1999; Johnson and Xie 2010). Note that the anomalous plus climatological SST field is computed by regressing annual ATL SST index with the SST field (Fig. S5), and then adding that to the climatological mean SST field. The precipitation

anomalies situated near the equator are the most important for remote teleconnections with deep atmospheric circulation, since the response to off-equatorial atmospheric heating is somewhat different (Gill 1980). Atmospheric heating over the tropical Atlantic has been shown to drive Kelvin-wave-induced wind anomalies that extend across the Indian and Central Pacific Oceans (Li et al. 2016). Despite the multi-model mean displaying very little signal (Fig. 9a), the individual models exhibit a vast array of differences to the observed behaviour. The region between the climatological and anomalous 27.5° C isotherms are situated in different regions, and in many cases, they do not align with their precipitation anomalies. This picture is in stark contrast to the AMIP simulations where the precipitation response is similar to observations (Fig. S6), which is consistent with the fact that the AMIP models are forced by observed SST. This coupled-model inconsistency underscores the likely role of anomalous SST gradients and a lack of surface wind convergence in the atmospheric response (e.g., Graham and Barnett 1987), which may not be simulated properly by the freely-evolving climate models. This implication is supported by our analysis which shows a strong tendency for models that simulate more realistic spatial structure of Atlantic SST anomalies (Fig. S5) to simulate more realistic precipitation anomalies (Fig. 9, 10c).

The background SST climatology also has the potential to play an important role in the precipitation response to anomalous SSTs, as it sets the location of the climatological 27.5° C isotherm and the background gradients (and surface wind divergence) that SST anomalies are imposed over. The pattern of mean SST shows that the models tend to be too warm off the coast of West Africa, and too cool off the Brazilian Coast up to the Caribbean Sea (Fig. S7). Hence the patterns of mean precipitation are also shifted. To first order, the observed tropical Atlantic SST climatology is characterised by warm waters to the north, and cooler water to the south (the mean tropical SST north of the equator in the ATL region is close to 2°C warmer than south of the equator; Fig. 10a). Thus, we have made the choice to analyse the model representation of the meridional SST gradient. We find that all but one model exhibits a weaker-than-observed meridional climatological SST gradient, and some are reversed. Overall, the models are too cool in the north and too warm in the south (Fig. S7), likely associated with the more southward position of the Intertropical Convergence Zone (ITCZ) compared to observations (Richter et al. 2014). Richter et al. (2014) linked the southward ITCZ bias to weaker-than-observed equatorial easterly winds, leading to warm bias in the equatorial eastern Atlantic. Note that our focus on meridional gradient SST is a different perspective to

328 the equatorial SST focus presented by Ritcher et al. (2014), whose analysis is confined to the region 2°S to
329 2°N; although their finding that models are generally too cool in the west and too warm in the east is not
330 inconsistent with ours. We find that models with a more realistic climatological SST gradient tend to also
331 simulate a more realistic range of 10-year trends in τ_{PAC} (Fig. 10b). Similarly, more realistic climatological
332 precipitation field over the Atlantic leads to improved range of 10-year τ_{PAC} trends (inter-model correlation
333 $r=0.34$, $p<0.05$; figure not shown). Hence, the representation of the tropical Atlantic climatology appears to
334 be important for the simulation of the decadal Pacific wind stress trends, through better representation of
335 atmospheric convection which is key for the atmospheric bridge mechanism. As noted earlier, where the
336 models simulate more realistic spatial structure of Atlantic SST anomalies, then they also tend to simulate a
337 more realistic pattern of precipitation anomalies (Fig. 10c). Precipitation is a proxy for convection in the
338 tropics, and hence improved precipitation response over the Atlantic might also indicate improved feedback
339 into the Pacific Walker Circulation cell.
340
341 ## 6. **Conclusion**
342 Variability of decadal trends in Pacific wind stress is under-represented in CMIP5 coupled models, despite
343 the fact that the magnitude of decadal SST variability is reasonably well simulated. Furthermore, the
344 relationship between the Atlantic-Pacific trans-basin SST gradient and the Pacific wind stress in models
345 agrees with observations. However, our study suggests that model biases over the tropical Atlantic are
346 largely to blame for the under-representation of Pacific wind stress trends. The correlation between decadal
347 Atlantic SST trends and the Pacific wind stress trends are the opposite to observations in most models.
348 Although the tropical Pacific SST is the dominant driver of the trade winds, the Atlantic state plays a role in
349 driving the wind trends to extreme values. Hence, our results suggest that the breakdown of the Atlantic-
350 Pacific connection in models leads to the under-representation of these extremes.
351
352 We examined both the climatological SST and anomalous SST biases over the tropical Atlantic. At the
353 outset, we found that in the AMIP experiments, the Pacific wind stress variations are reasonably well
354 recovered. Therefore, given the particular observed configuration of the climatological and anomalous SST
355 fields, the atmosphere models are able to simulate the range of the wind stress trends. McGregor et al. (2014)
356 find that, in the AMIP multi-model trend over 1992 to 2011, the zonal wind at 850hPa is in stronger

agreement with observations than at the surface, attributing the difference to a deficiency in the downward mixing of momentum. Exploration of the winds at various atmospheric levels in the historical CMIP5 simulations may uncover further interesting features. However, our inter-model analysis indicates that the Pacific trade wind trend variability is improved where the Atlantic SST climatology bias is reduced in the coupled models. Furthermore, we found that the Atlantic precipitation response is improved where the pattern of Atlantic SST anomalies is more like observations. Since precipitation is a proxy for convection, we infer that the coupled models are deficient at generating the convective processes that would otherwise drive the descending branch of the Walker Circulation over the tropical Atlantic. Without this feedback into the Walker Circulation, there is an absence of a connection to the Pacific trade winds, which are the surface level expression of the Pacific Walker Circulation cell.

A confounding factor in this inter-model study is that models present biases in different ways and locations. For example, the north, south, and equatorial Atlantic regions are known to have differing influences on decadal Pacific dynamics (Chikamoto et al. 2016). Hence, although a particular model may perform well in one region, it might be masked by stronger biases in another region. We will examine this issue in a future study by running model experiments with a range of SST configurations, but in particular, with the biased CMIP5 multi-model mean Atlantic SST climatology, in a partially coupled climate model. These experiments will allow us to more deeply understand how the Atlantic SST climatology is connected to the range of the Pacific trade wind trends.

References

Chikamoto, Y. *et al.* Skilful multi-year predictions of tropical trans-basin climate variability. *Nat. Commun.* **6,** 6:6869 (2015).

Chikamoto, Y., Mochizuki, T., Timmermann, A., Kimoto, M. & Watanabe, M. Potential tropical Atlantic impacts on Pacific decadal climate trends. *Geophys. Res. Lett.* **43,** 7143–7151 (2016).

Compo, G. P. *et al.* The Twentieth Century Reanalysis Project. *Q. J. R. Meteorol. Soc.* **137,** 1–28 (2011).

Douville, H., Voldoire, A. & Geoffroy, O. The recent global warming hiatus: What is the role of Pacific variability? *Geophys. Res. Lett.* **42,** 880–888 (2015).

England, M. H. *et al.* Recent intensification of wind-driven circulation in the Pacific and the ongoing warming hiatus. *Nat. Clim. Chang.* **4,** 222–227 (2014).

England, M. H., Kajtar, J. B. & Maher, N. Robust warming projections despite the recent hiatus. *Nat. Clim. Chang.* **5,** 394–396 (2015).

Gill, A. E. Some simple solutions for heat-induced tropical circulation. *Q. J. R. Meteorol. Soc.* **106,** 447–462 (1980).

Graham, N. E. & Barnett, T. P. Sea surface temperature, surface wind divergence, and convection over tropical oceans. *Science* **238**, 657–659 (1987).

Henley, B. J. *et al*. Spatial and Temporal Agreement in Climate Model Simulations of the Interdecadal Pacific Oscillation. *Environ. Res. Lett*. at press, doi:10.1088/1748-9326/aa5cc8 (2017).

Huang, B., Banzon, V.F., Freeman, E., Lawrimore, J., Liu, W., Peterson, T.C., Smith, T.M., Thorne, P.W., Woodruff, S.D., and Zhang, H.-M. Extended Reconstructed Sea Surface Temperature version 4 (ERSST.v4): Part I. Upgrades and intercomparisons. *J. Clim.* **28**, 911–930 (2014).

Johnson, N. C. & Xie, S.-P. Changes in the sea surface temperature threshold for tropical convection. *Nat. Geosci.* **3,** 842–845 (2010).

Kajtar, J. B., Santoso, A., England, M. H. & Cai, W. Tropical climate variability: interactions across the Pacific, Indian, and Atlantic Oceans. *Clim. Dyn.* **48,** 2173–2190 (2017).

Kalnay E. *et al*. The NCEP/NCAR 40-year reanalysis project. *Bull. Amer. Meteor. Soc.,* **77**, 437-470 (1996).

Kociuba, G. & Power, S. B. Inability of CMIP5 models to simulate recent strengthening of the walker circulation: Implications for projections. *J. Clim.* **28,** 20–35 (2015).

Kucharski, F., Kang, I. S., Farneti, R. & Feudale, L. Tropical Pacific response to 20th century Atlantic warming. *Geophys. Res. Lett.* **38,** L03702 (2011).

Kucharski, F. *et al.* Atlantic forcing of Pacific decadal variability. *Clim. Dyn.* **46,** 2337–2351 (2016a).

Kucharski, F. *et al.* The Teleconnection of the Tropical Atlantic to Indo-Pacific Sea Surface Temperatures on Inter-Annual to Centennial Time Scales: A Review of Recent Findings. *Atmosphere (Basel).* **7,** 29 (2016b).

L'Heureux, M. L., Lee, S. & Lyon, B. Recent multidecadal strengthening of the Walker circulation across the tropical Pacific. *Nat. Clim. Chang.* **3,** 571–576 (2013).

Lau, N.-C. & Nath, M. J. A modeling study of the relative roles of tropical and extratropical SST anomalies in the variability of the global atmosphere-ocean system. *J. Clim.* **7,** 1184–1207 (1994).

Lee, S.-K. *et al.* Pacific origin of the abrupt increase in Indian Ocean heat content during the warming hiatus. *Nat. Geosci.* **8,** 445–449 (2015).

Li, X., Xie, S.-P., Gille, S. T. & Yoo, C. Atlantic-induced pan-tropical climate change over the past three decades. *Nat. Clim. Chang.* **6,** 275–280 (2016).

Lin, J. L. The double-ITCZ problem in IPCC AR4 coupled GCMs: Ocean-atmosphere feedback analysis. *J. Clim.* **20,** 4497–4525 (2007).

Luo, J.-J., Sasaki, W. & Masumoto, Y. Indian Ocean warming modulates Pacific climate change. *Proc. Natl. Acad. Sci. U. S. A.* **109,** 18701–6 (2012).

Ma, S. & Zhou, T. Robust strengthening and westward shift of the tropical Pacific Walker circulation during 1979-2012: a comparison of 7 sets of reanalysis data and 26 CMIP5 models. *J. Clim.* **29,** 3097–3118 (2016).

McGregor, S. *et al.* Recent Walker circulation strengthening and Pacific cooling amplified by Atlantic warming. *Nat. Clim. Chang.* **4,** 888–892 (2014).

Mochizuki, T., Kimoto, M., Watanabe, M., Chikamoto, Y. & Ishii, M. Inter-basin effects of the Indian Ocean on Pacific decadal climate change. *Geophys. Res. Lett.* **43,** 7168–7175 (2016).

Poli, P. *et al.* ERA-20C: An atmospheric reanalysis of the 20th century. *J. Clim.* **29,** 4083–4097 (2016).

Power, S. B., & Kociuba, G. What caused the observed Twentieth-Century weakening of the Walker Circulation? *J. Clim.* **24**, 6501–6514 (2011).

Rayner, N. A. *et al.* Global analyses of sea surface temperature, sea ice, and night marine air temperature since the late nineteenth century. *J. Geophys. Res.* **108,** 4407 (2003).

Richter, I., Xie, S. P., Behera, S. K., Doi, T. & Masumoto, Y. Equatorial Atlantic variability and its relation to mean state biases in CMIP5. *Clim. Dyn.* **42,** 171–188 (2014).

Ruprich-Robert, Y., Castruccio, F., Msadek, R., Yeager, S. G., Delworth, T. L., & Danabasoglu, G. Assessing the climate impacts of the observed Atlantic Multidecadal Variability using the GFDL CM2 .1 and NCAR CESM1 global coupled models. *J. Clim.* at press, doi:10.1175/JCLI-D-16-0127.1, (2016).

Sud, Y. C., Walker, G. K. & Lau, K-M. Mechanisms regulating sea-surface temperatures and deep convection in the tropics. Geophys. Res. Lett. 26, 1019–1022 (1999).

Takahashi, C. & Watanabe, M. Pacific trade winds accelerated by aerosol forcing over the past two decades. *Nat. Clim. Chang.* **6,** 768–774 (2016).

Toniazzo, T. & Woolnough, S. Development of warm SST errors in the southern tropical Atlantic in CMIP5 decadal hindcasts. *Clim. Dyn.* **43,** 2889–2913 (2014).

Vecchi, G. A. *et al.* Weakening of tropical Pacific atmospheric circulation due to anthropogenic forcing. *Nature* **441,** 73–76 (2006).

Vecchi, G. A. & Soden, B. J. Global Warming and the Weakening of the Tropical Circulation. *J. Clim.* **20,** 4316–4340 (2007).

Zhang, C. Large-scale variability of atmospheric deep convection in relation to sea surface temperature in the tropics. J. Clim. **6**, 1898–1913 (1993).

Zhang, L., & Karnauskas, K. B. The Role of Tropical Interbasin SST Gradients in Forcing Walker Circulation Trends. *J. Clim.* **30**, 499–508 (2017).

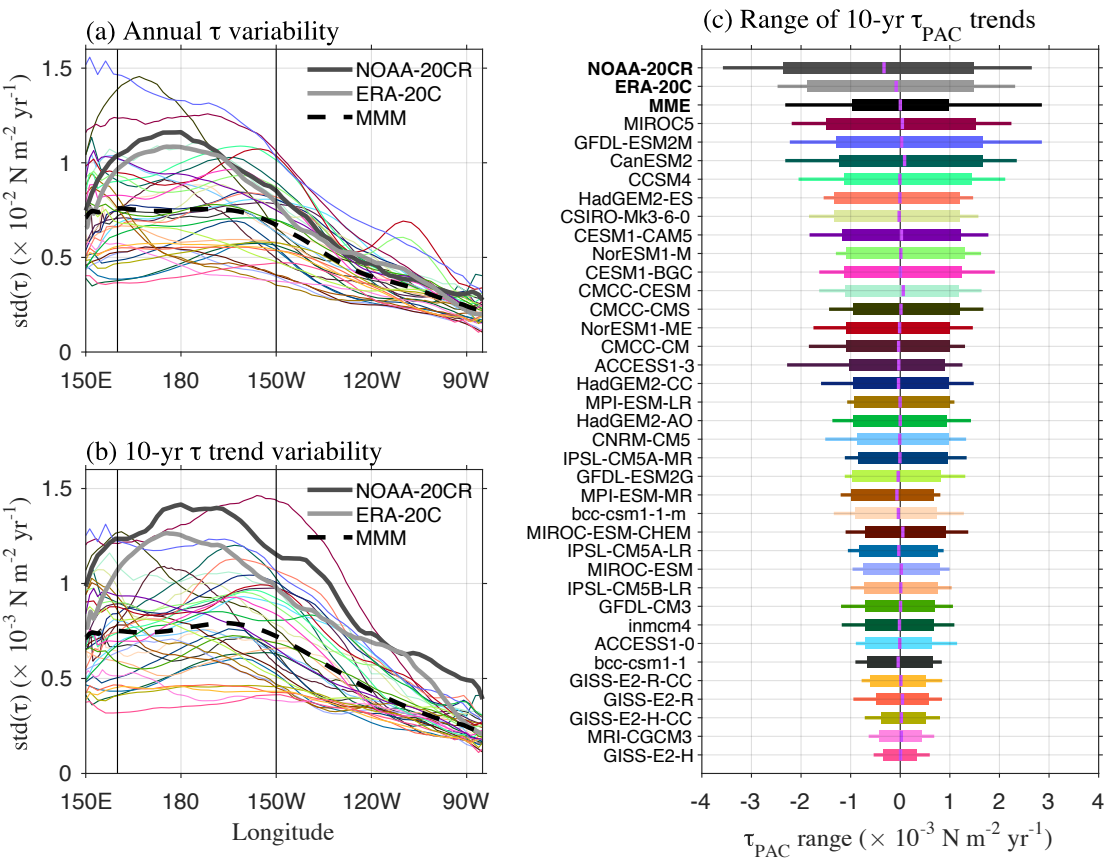

Fig. 1 Variability of Pacific zonal wind stress, in CMIP5 models and observations. a, Equatorial mean of the standard deviation of annual zonal wind stress (τ) averaged over 8°S to 8°N, shown only for the Pacific sector. **b**, As in **a**, but for the standard deviation of running 10-year zonal wind stress trends. **c**, The range of 10-year trends in the τ_{PAC} index (zonal wind stress averaged over 160°E – 150°W and 8°S – 8°N, as indicated by the vertical lines in **a** and **b**). MMM (in **a** and **b**) denotes the multi-model mean. MME (in **c**) denotes the range of the multi-model ensemble. The widths of the bars (in **c**) denote the 5% to 95% intervals, and the whiskers denote the full range. Vertical purple dashes denote the mean trend. The individual models are ordered by the width of the 90% intervals.

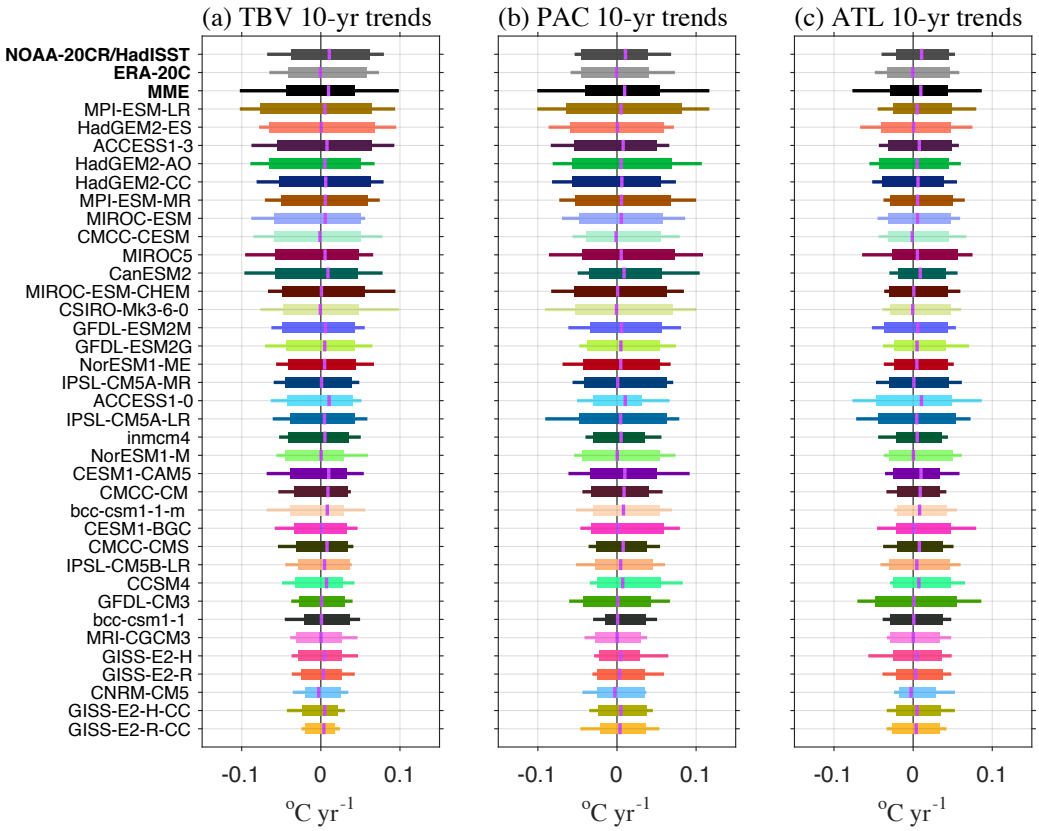

Fig. 2 Range in 10-year trends of SST indices, in CMIP5 models and observations. a, Trans-basin variability index (tropical Atlantic minus the tropical Pacific SST index). **b**, Tropical Pacific index (SST averaged over 120°E – 90°W and 20°S – 20°N). **c**, Tropical Atlantic index (SST averaged over 70°W – 20°E and 20°S – 20°N). MME denotes the ranges of the multi-model ensemble. The widths of the bars denote the 5% to 95% intervals, and the whiskers denote the full range. Vertical purple dashes denote the mean trend. The individual models are ordered by the range of TBV.

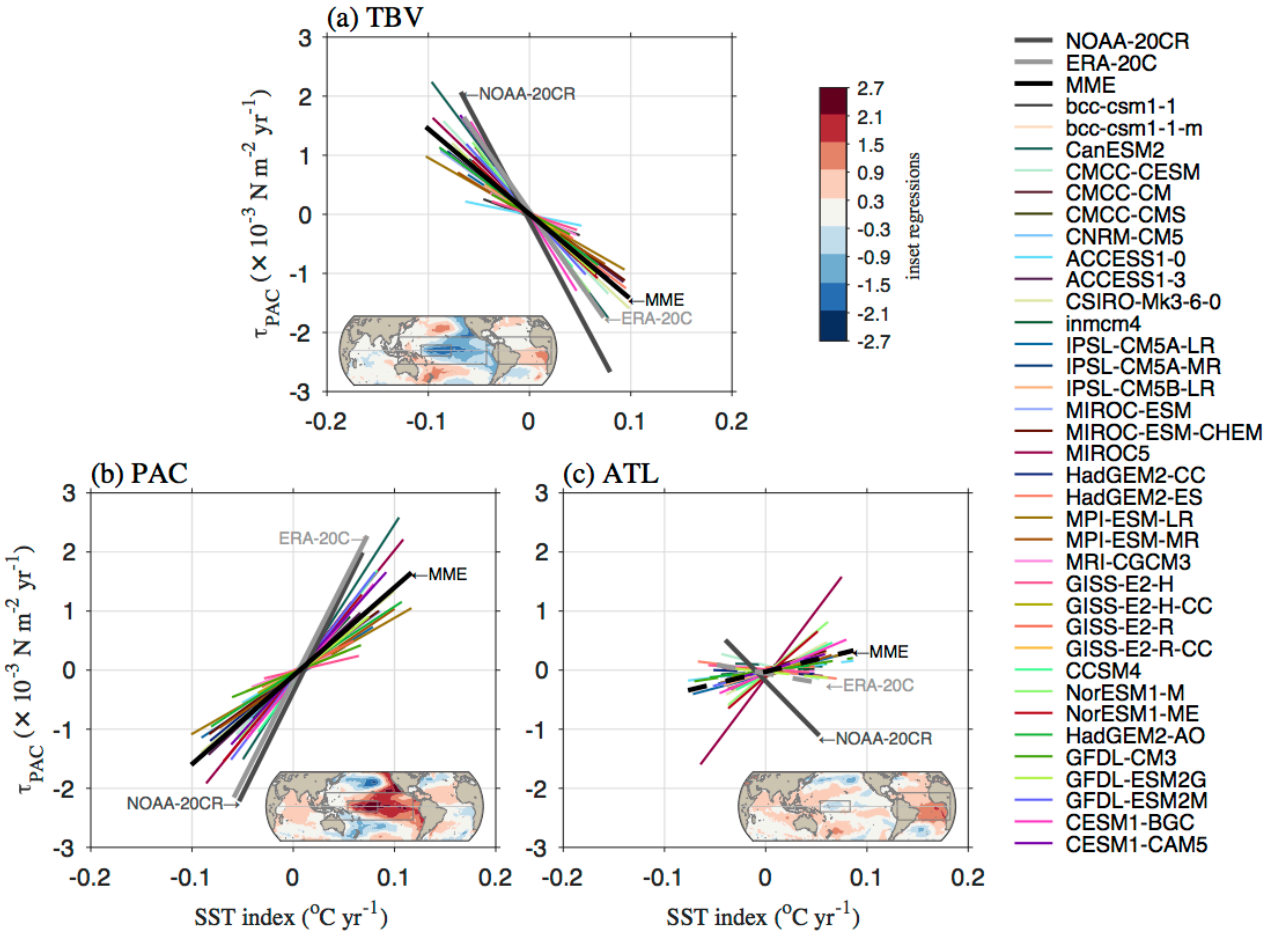

Fig. 3 Regression lines of 10-year trends in the Pacific wind stress index (τ_{PAC}) against various SST indices (TBV, PAC, and ATL), in CMIP5 models and observations. a, Trans-basin variability index (TBV). **b**, Tropical Pacific index (PAC). **c**, Tropical Atlantic index (ATL). The lines are terminated at the minimum and maximum values of the respective SST index trends. Solid lines indicate a statistically significant regression at the 95% level, and broken lines indicate otherwise. The inset in each panel is the running 10-year trends of the corresponding SST indices regressed with the SST field trends in HadISST. The grey rectangles in the insets denote the area of the SST and τ_{PAC} indices.

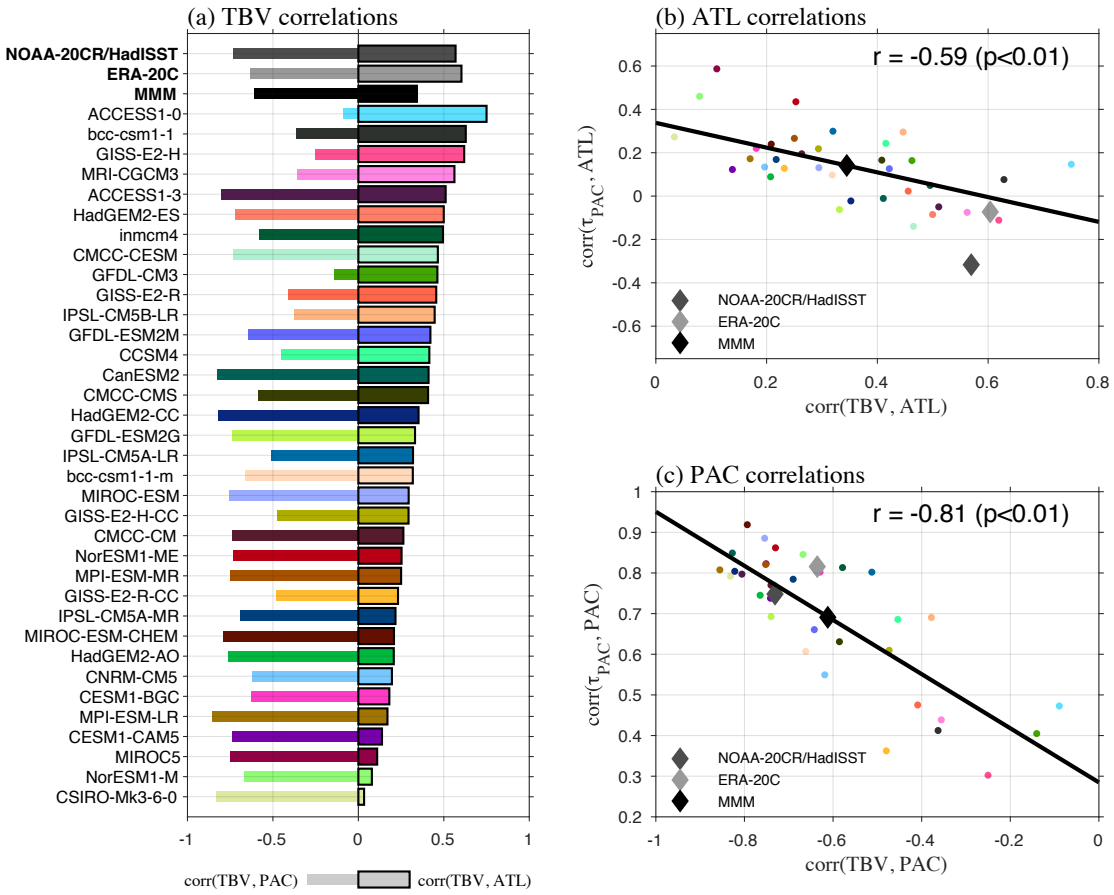

40

41 **Fig. 4 Correlations between 10-year trends of Pacific wind stress and SST indices, in CMIP5 models**
42 **and observations. a**, Trans-basin variability index correlations with the tropical Atlantic and tropical
43 Pacific SST indices. **b**, Relationship across models and observations between the TBV-ATL and the τ_{PAC}-
44 ATL (Fig. S2) correlation coefficients. **c**, Relationship across models and observations between the TBV-
45 PAC and the τ_{PAC}-PAC (Fig. S2) correlation coefficients. In **b** and **c**, the inter-model correlation and
46 corresponding p-values are quoted in the top right of the panel.

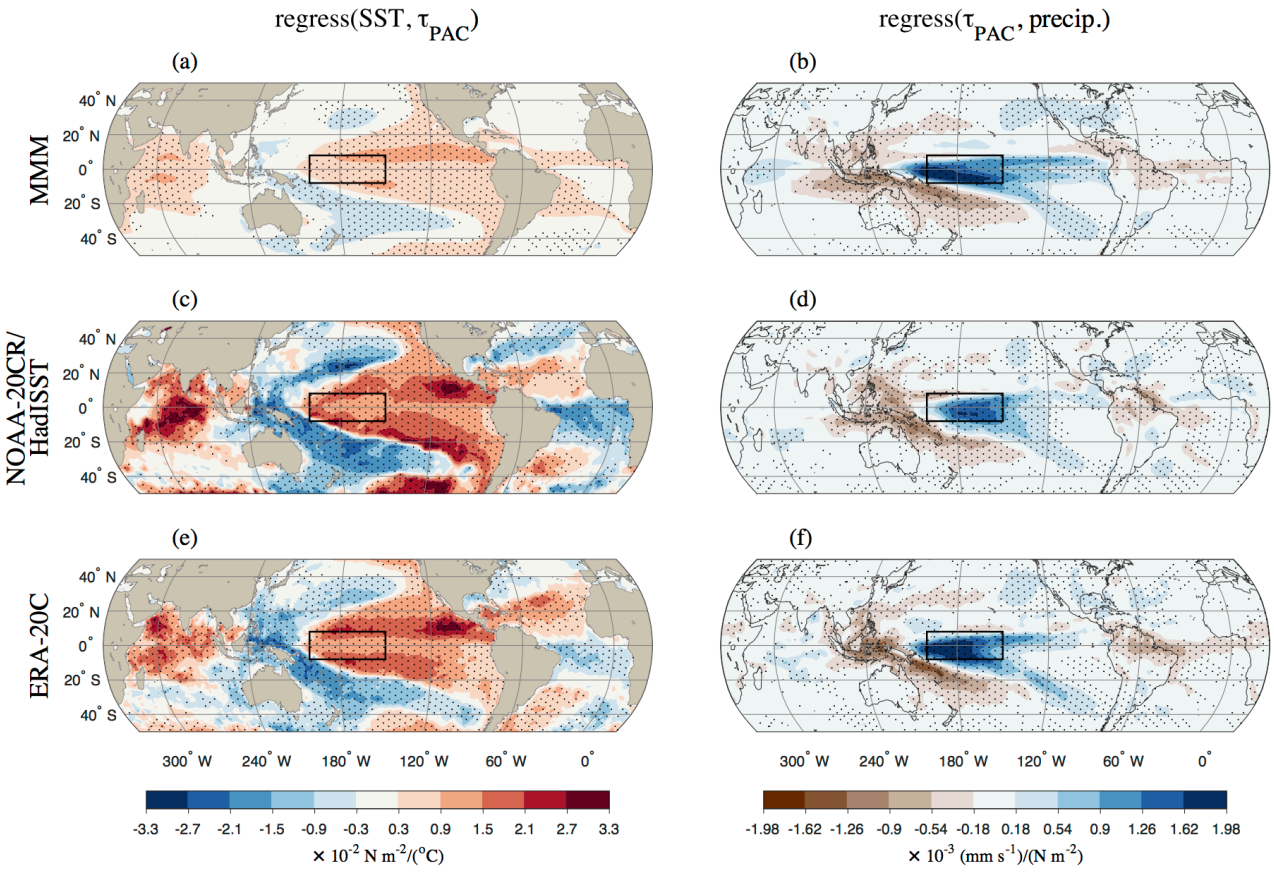

Fig. 5 Running 10-year trends of the Pacific wind stress regressed with SST and precipitation trends, in CMIP5 models and observations. a, Multi-model mean regression of running 10-year τ_{PAC} trends with SST field trends. **b**, Multi-model mean regression of running 10-year τ_{PAC} trends with precipitation field trends. Note that the regression in **a** is performed such that the plot represents the τ_{PAC} response per unit temperature at each grid-point (and thus consistent with Fig. 3), whereas the regression in **b** shows the precipitation response per unit τ_{PAC}. **c**,**d**, As in **a** and **b**, but for NOAA 20CR wind stress and precipitation, and HadISST sea surface temperature. **e**,**f,** As in **a** and **b**, but for ERA 20C. For the multi-model means in **a** and **b**, the stippling denotes regions where at least 75% of the models agree on the sign on the regression. For the reanalysis products in **c**–**f**, the stippling denotes statistically significant regression coefficients at 95% confidence level.

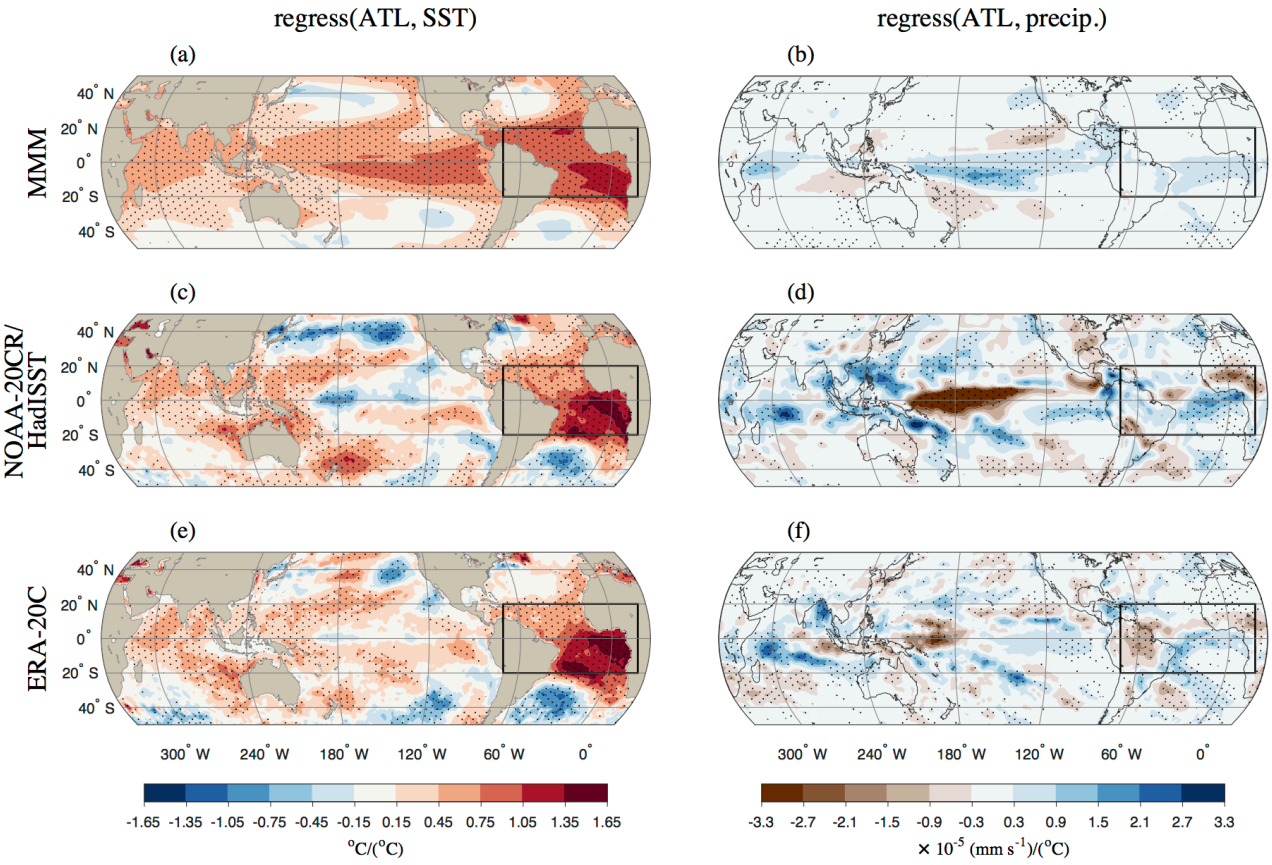

Fig. 6 Running 10-year trends of the Atlantic SST index (ATL) regressed with SST and precipitation trends, in CMIP5 models and observations. a, Multi-model mean regression of running 10-year ATL trends with SST field trends. **b**, Multi-model mean regression of running 10-year ATL trends with precipitation field trends. **c**,**d**, As in **a** and **b**, but for NOAA 20CR precipitation, and HadISST sea surface temperature. **e**,**f,** As in **a** and **b**, but for ERA 20C. Stippling denotes the same as in Fig. 5.

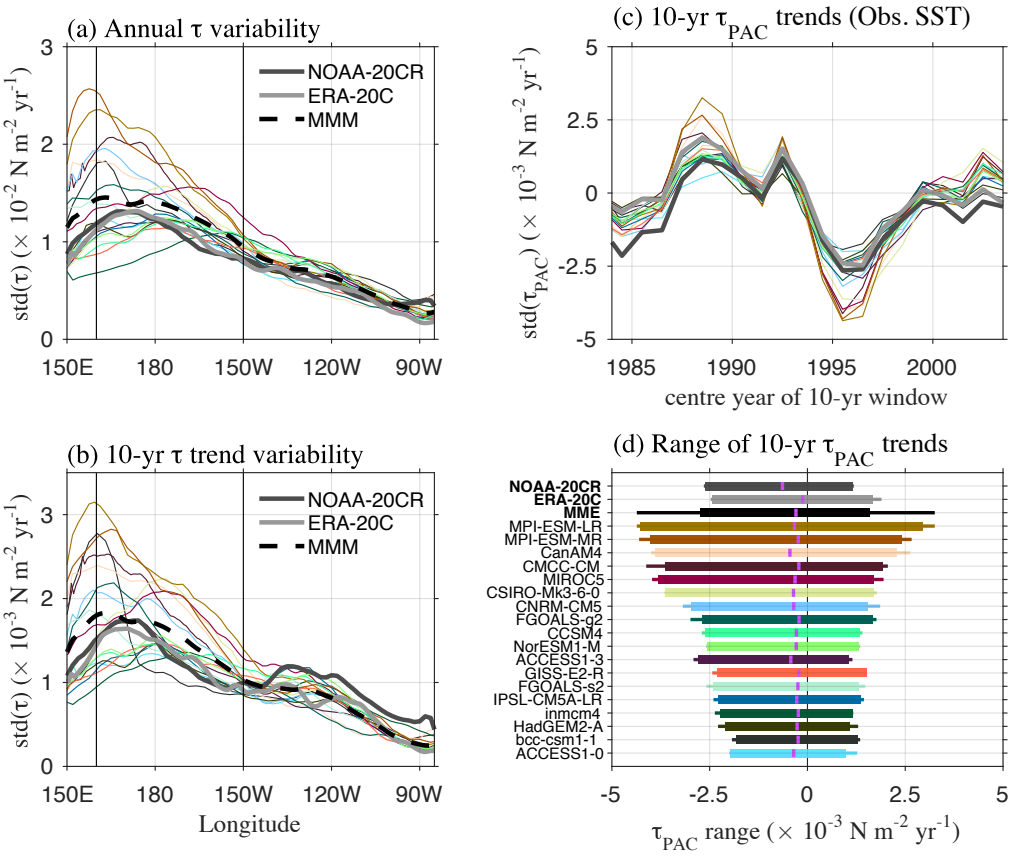

Fig. 7 Variability of Pacific zonal wind stress, in AMIP models and observations. Only the period 1979-2008 is considered, corresponding to the span of the AMIP experiments. **a**, Equatorial mean of the standard deviation of annual zonal wind stress (τ) averaged over 8°S to 8°N, shown only for the Pacific sector. **b**, As in **a**, but for the standard deviation of running 10-year zonal zonal wind stress trends. **c**, Time-series of running 10-year trends in the τ_{PAC} index. **d**, The range of 10-year trends in the τ_{PAC} index. MMM (in **a** and **b**) denotes the multi-model mean. MME (in **d**) denotes the range of the multi-model ensemble. The widths of the bars (in **d**) denote the 5% to 95% intervals, and the whiskers denote the full range. Vertical purple dashes denote the mean trend. The individual models are ordered by the width of the 90% intervals.

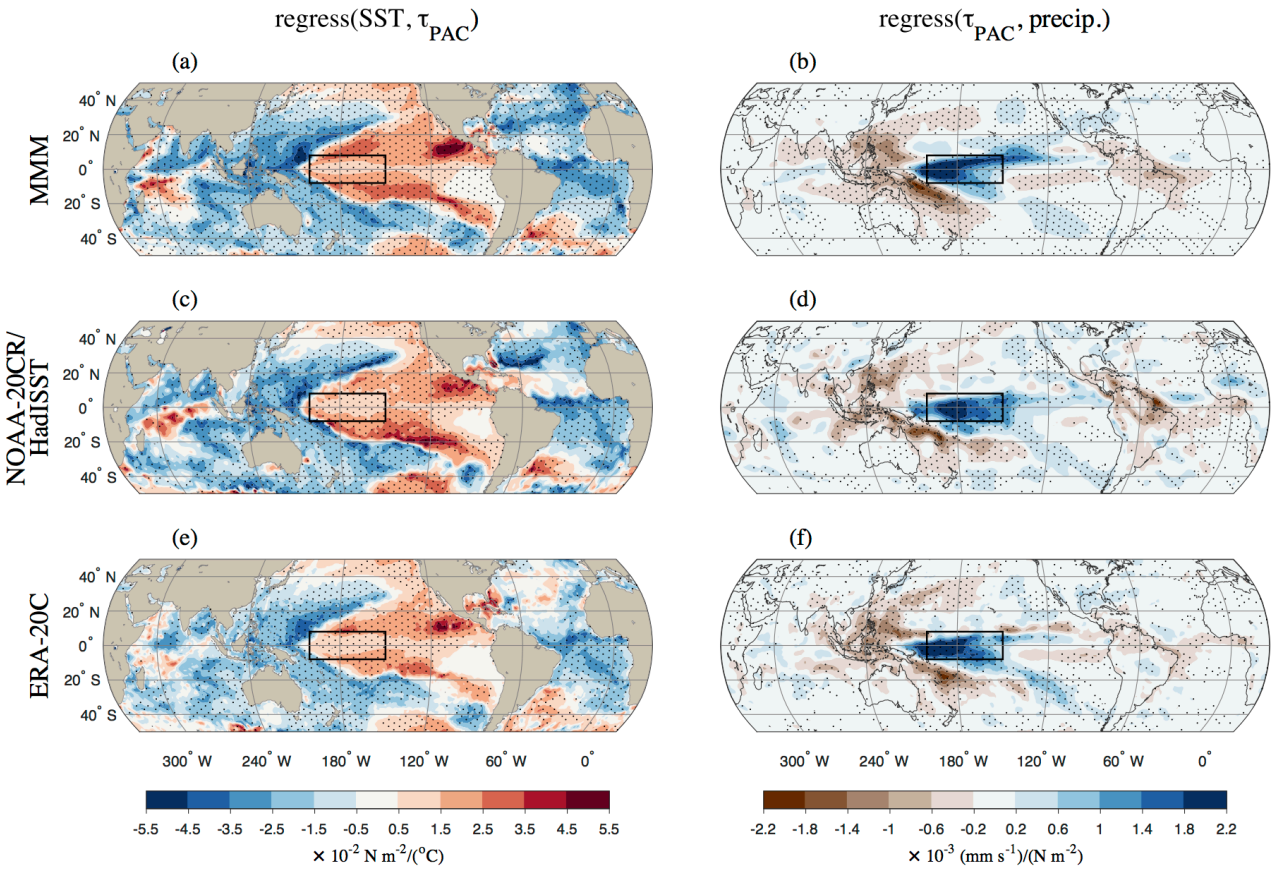

Fig. 8 Running 10-year trends of the Pacific wind stress regressed with SST and precipitation fields, in AMIP models and observations. Only the period 1979-2008 is considered, corresponding to the span of the AMIP experiments. **a**, Multi-model mean regression of running 10-year τ_{PAC} trends with observed SST field trends. **b**, Multi-model mean regression of running 10-year τ_{PAC} trends with precipitation field trends. Note that the regressions are computed in the same way as for Fig. 5. **c**,**d**, As in **a** and **b**, but for NOAA 20CR wind stress and precipitation, and HadISST sea surface temperature. **e**,**f,** As in **a** and **b**, but for ERA 20C. Stippling denotes the same as in Fig. 5.

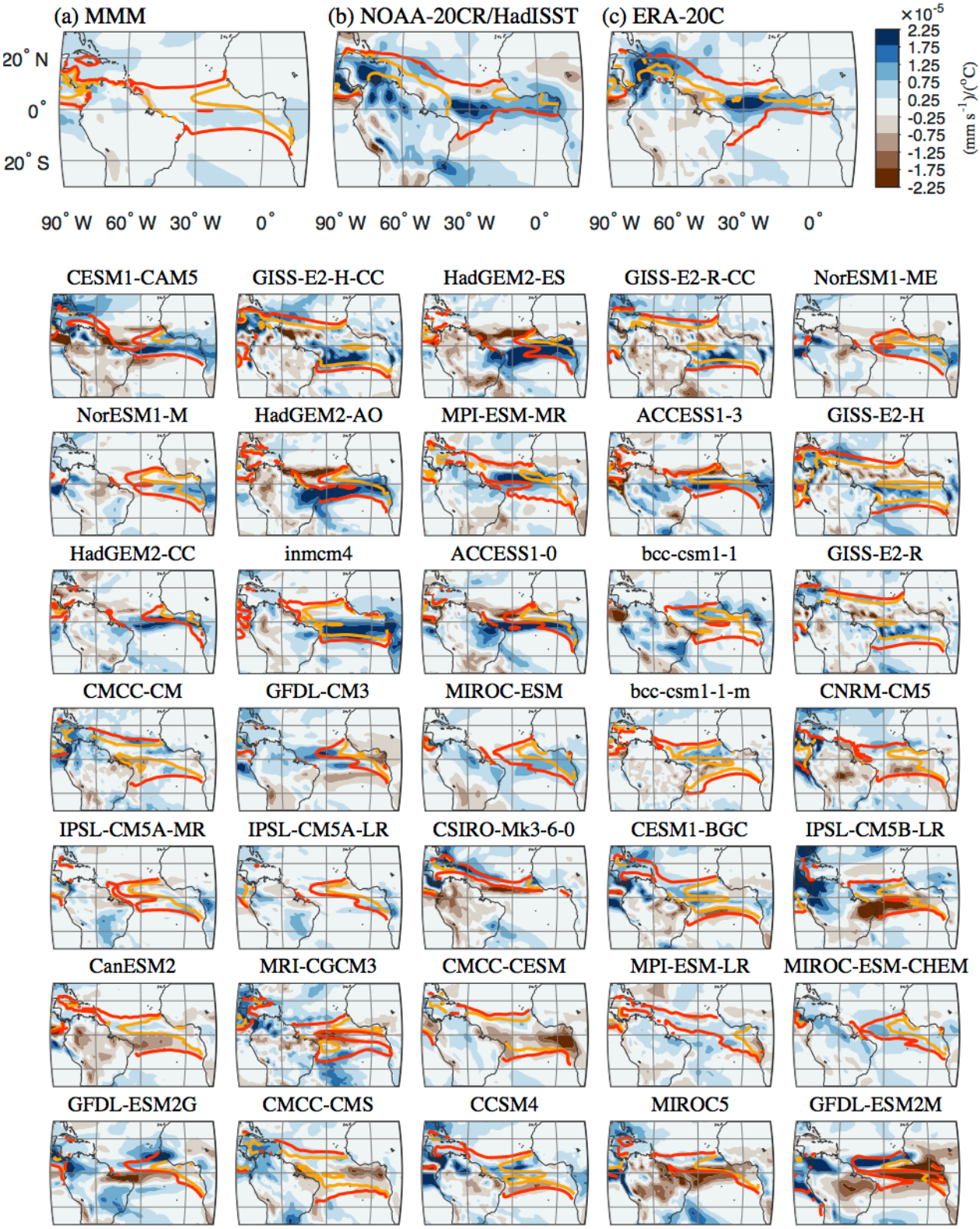

Fig. 9 Annual ATL SST index regressed with precipitation, in CMIP5 models and observations. **a**, Multi-model mean of the regression of annual ATL SST indices with precipitation fields. **b**, Annual HadISST ATL index regressed with NOAA 20CR precipitation field. **c**, Annual ATL index regressed with precipitation field in ERA 20C. The remaining panels are the same as **a**–**c**, but for each individual CMIP5 model. The models are ordered by strongest correlation with the mean of the two observed fields of ATL

index regression with SST (Fig. S5b, c). The yellow contours denote the 27.5° C isotherm of the climatological SST. The orange contours denote the 27.5° C isotherm of the anomalous SST field plus the climatological SST. The anomalous SST field is computed by regressing annual ATL index with SST (Fig. S5).

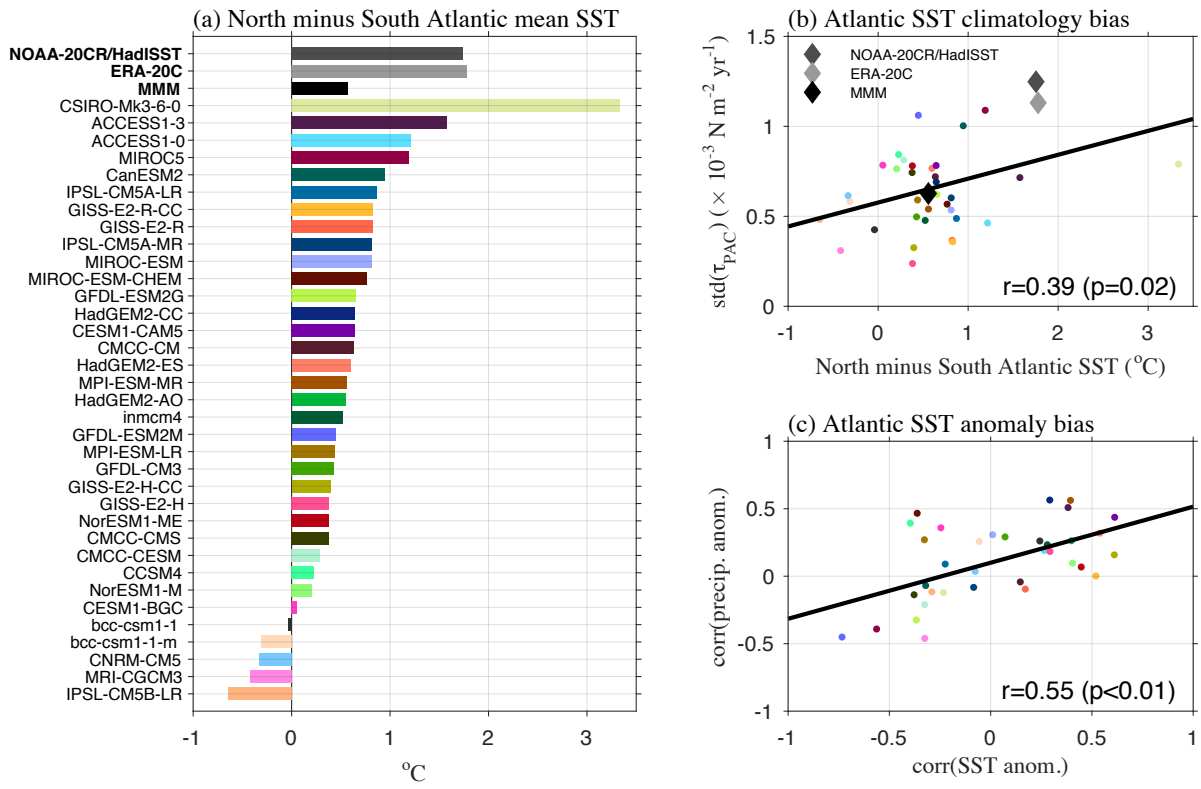

92

93 **Fig. 10 Atlantic SST biases, and their influence on Pacific wind stress trends and Atlantic**
94 **precipitation. a**, Climatological mean North Atlantic SST (averaged over 70°W – 20°E and 20°S – 0°)
95 minus mean South Atlantic SST (averaged over 70°W – 20°E and 0° – 20°N). **b**, Inter-model relationship
96 between north minus south Atlantic SST, and the standard deviation of τ_{PAC} 10-yr trends. **c**, Inter-model
97 relationship between the model versus observation correlation of Atlantic SST anomalies and the model
98 versus observation correlation of Atlantic precipitation anomalies. The Atlantic anomalous SST field is
99 computed by regressing the ATL index with SST (Fig. S5), and the Atlantic anomalous precipitation field
100 by regressing the ATL index with precipitation (Fig. 9). The correlation coefficients and corresponding p-
101 values are quoted in the bottom right corners of **b** and **c**.

Model under-representation of decadal Pacific trade wind trends and its link to tropical Atlantic bias

Jules B. Kajtar*[1,2,3], Agus Santoso[1,2], Shayne McGregor[1,4], Matthew H. England[1,2], and Zak Baillie[1,2]

[1] Australian Research Council's Centre of Excellence for Climate System Science, Sydney, Australia
[2] Climate Change Research Centre, University of New South Wales, Sydney, NSW, Australia
[3] Present Address: College of Engineering, Mathematics, and Physical Sciences, University of Exeter, Exeter, UK
[4] School of Earth, Atmosphere and Environment, Monash University, Melbourne, VIC, Australia

* Corresponding author: j.kajtar@exeter.ac.uk.

Supplementary Material

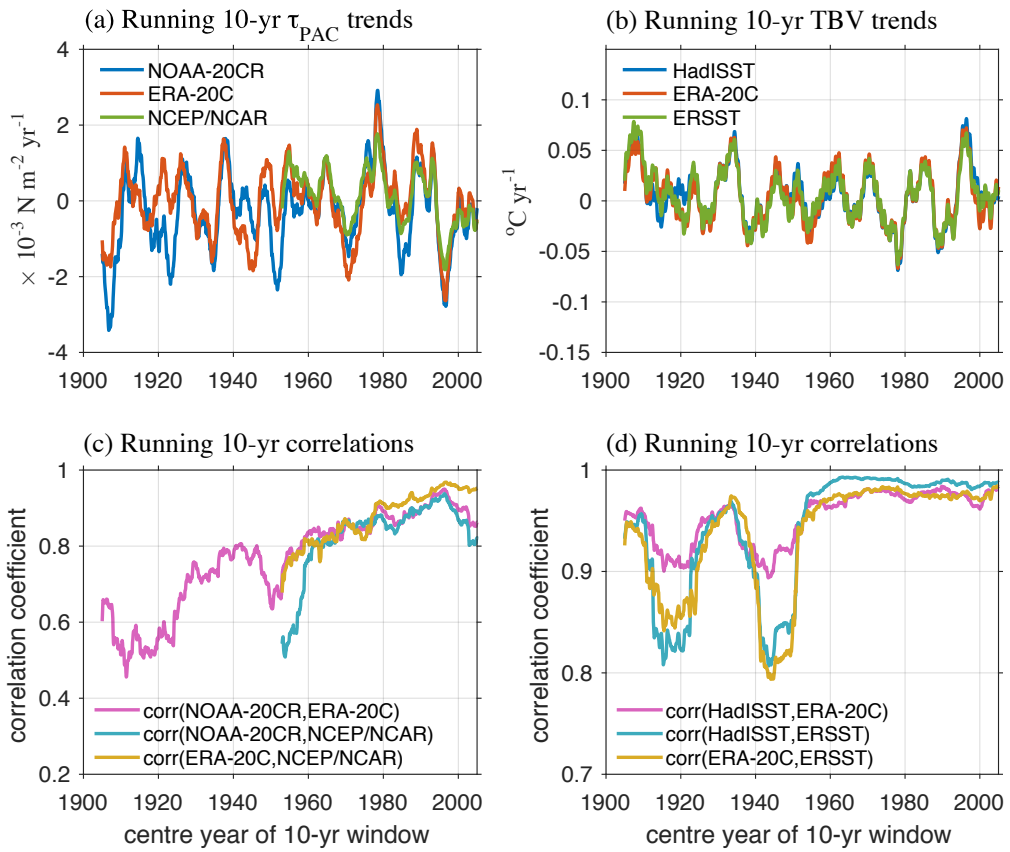

Fig. S1 Running 10-year trends of the Pacific wind stress (τ_{PAC}) and trans-basin variability (TBV) indices, in a range of reanalysis products. **a** Running trends of Pacific wind stress index (τ_{PAC}). **b** Running trends of trans-basin variability SST index. **c** Running correlations in 10-year windows between τ_{PAC} from different products. **d** Running correlations in 10-year windows between TBV from different products.

Fig. S2 Correlations between 10-year running trends in the Pacific wind stress index and SST indices, in CMIP5 models and observations. The SST indices are: the trans-basin variability index (TBV), the tropical Pacific index (PAC), and the tropical Atlantic index (ATL). The *red vertical lines* indicate the level beyond which the correlations are statistically significant at the 95% level. MMM denotes the multi-model mean correlations.

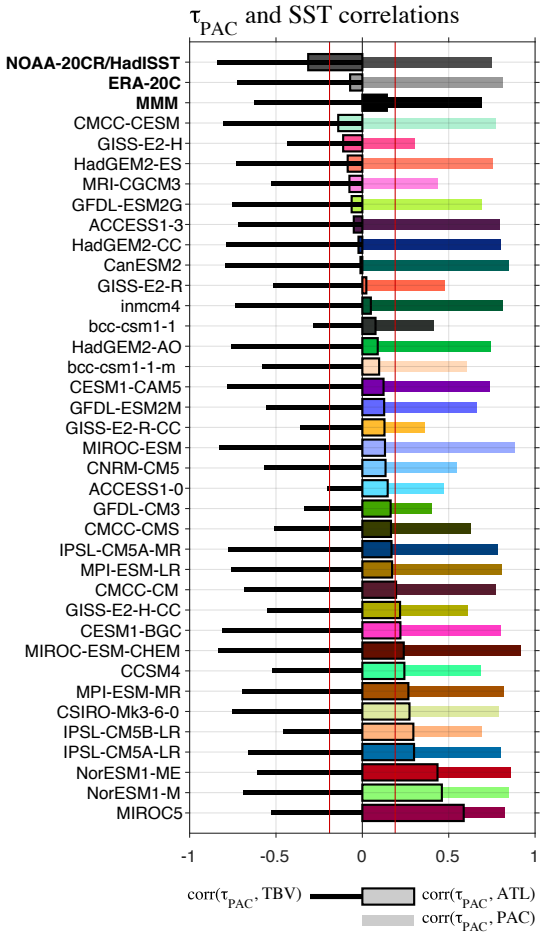

Fig. S3 Regression lines of 10-year trends in the Pacific wind stress index (τ_{PAC}) against the Indian Ocean SST index (IND), in CMIP5 models and observations. The *lines* are terminated at the minimum and maximum values of the IND index trends. *Solid lines* indicate a statistically significant regression at the 95% level, and *broken lines* indicate otherwise. The inset is the running 10-year IND trends regressed with the SST field trends in HadISST. The *grey rectangles* in the inset denote the area of the IND and τ_{PAC} indices.

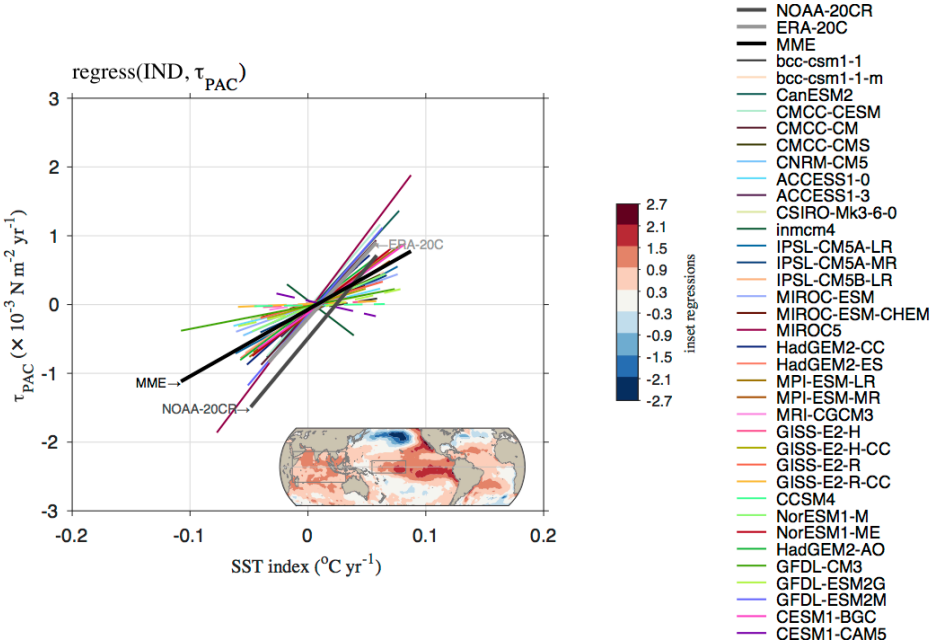

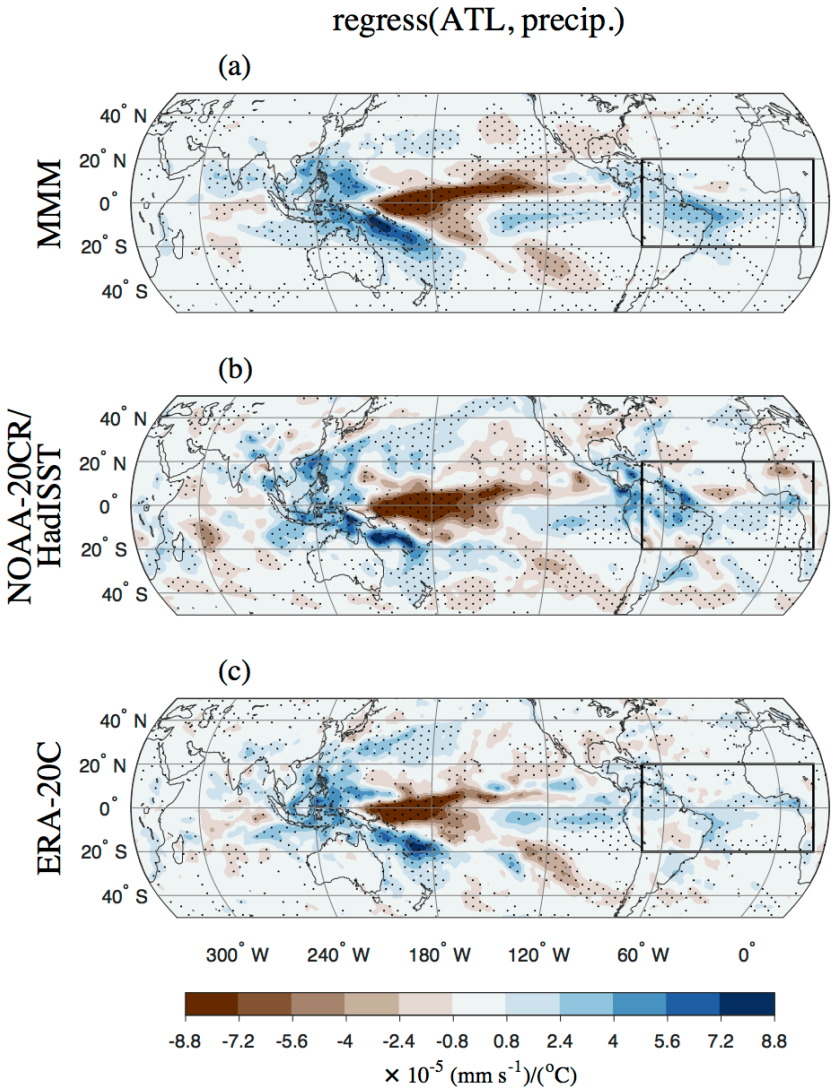

Fig. S4 Running 10-year trends of the ATL SST index regressed with precipitation trends, in AMIP models and observations. Only the period 1979-2008 is considered, corresponding to the span of the AMIP experiments. **a** Multi-model mean regression of running 10-year ATL trends with precipitation field trends. **b** As in **a**, but for NOAA-20CR precipitation and HadISST ATL index. **c** As in **a**, but for ERA-20C. *Stippling* denotes the same as in Fig. 5.

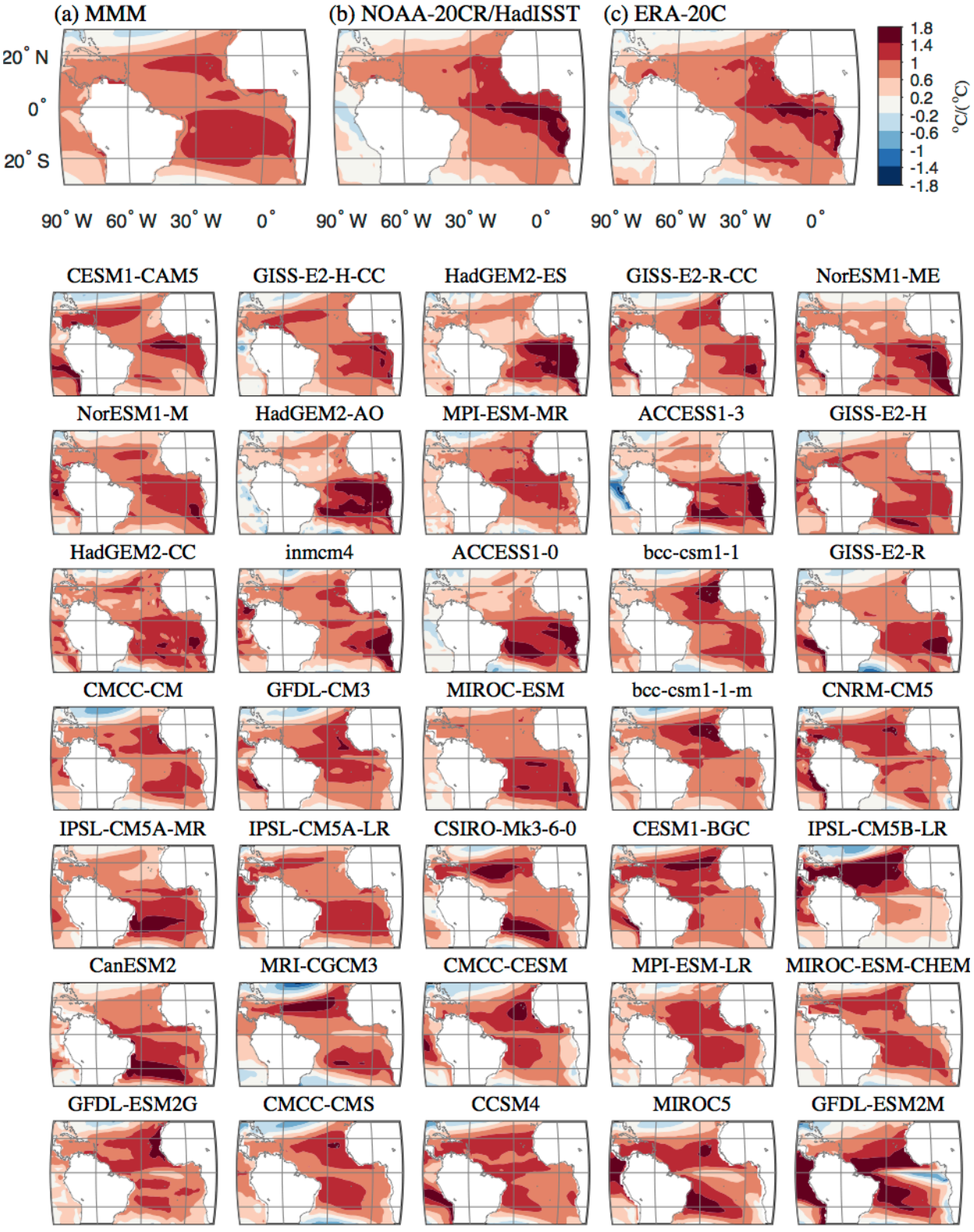

Fig. S5 Annual ATL SST index regressed with SST fields, in CMIP5 models and observations. **a** Multi-model mean of the regression of annual ATL SST indices with SST fields. **b** HadISST regression. **c** ERA-20C regression. The remaining panels are the same as **a**–**c**, but for each individual CMIP5 model. The models are ordered by strongest correlation with the mean of the two observed SST regression fields (**b** and **c**).

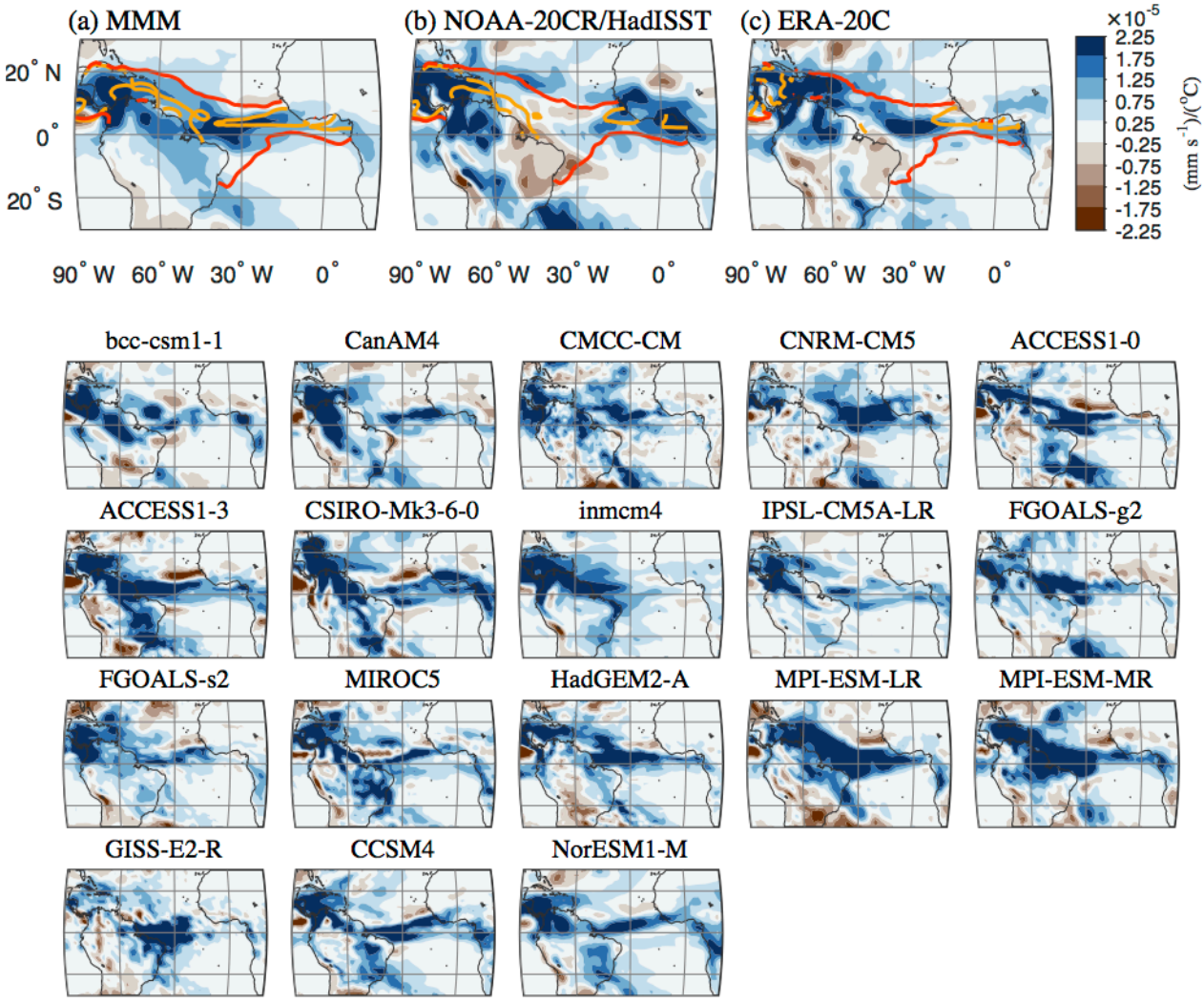

Fig. S6 Annual ATL SST index regressed with precipitation, in AMIP models and observations. Only the period 1979-2008 is considered, corresponding to the span of the AMIP experiments. **a** Multi-model mean regression of annual ATL SST indices with precipitation fields. **b** Annual HadISST ATL index regressed with NOAA-20CR precipitation field. **c** Annual ATL index regressed with precipitation field in ERA-20C. The remaining panels are the same as **a**–**c**, but for each individual AMIP model. The *yellow contours* in **a**–**c** denote the 27.8° C isotherm of the climatological SST. The *orange contours* in **a**–**c** denote the 27.8° C isotherm of the anomalous SST field plus the climatological SST (as in Fig. 8). The isotherm contours have been omitted from the individual model panels, since they are identical to those in **a**. Note that we have selected the 27.8° C isotherms here (as opposed to 27.5° C like Fig. 9) since the climatological mean SST is generally warmer for this recent period than over the entire twentieth century. Precipitation in the tropical region occurs over a threshold that is assumed to be a function of the mean tropical temperature (Johnson & Xie, 2010).

Fig. S7 Atlantic climatological mean SST and precipitation fields, in CMIP5 models and observations. **a** Multi-model mean SST and precipitation fields. **b** NOAA-20CR precipitation and HadISST mean fields. **c** ERA-20C mean fields. The *colour shading* denotes SST and the *overlaid contours* denote the mean precipitation (mm/day).